INTERNATIONAL JOURNAL OF CLIMATOLOGY
Int. J. Climatol. **32**: 1406–1422 (2012)
Published online 14 June 2011 in Wiley Online Library
(wileyonlinelibrary.com) DOI: 10.1002/joc.2363

RMetS
Royal Meteorological Society

High-resolution analysis of daily precipitation trends in the central Alps over the last century

Y. Brugnara,[a] M. Brunetti,[a]* M. Maugeri,[a,b] T. Nanni[a] and C. Simolo[a]
[a] *ISAC-CNR, I-40129 Bologna, Italy*
[b] *Dipartimento di Fisica, Università degli Studi di Milano, I-20133 Milano, Italy*

ABSTRACT: In this work we present a homogenized high-resolution data set composed of 200 daily precipitation series spanning the last 90 years, located over an area centred on the Trentino – South Tyrol region (central part of the European Alps), in a transition zone between the climates of the southern and northern slopes of the Alps. We analysed the trends of total precipitation (TP), wet days (WD) and average intensity (PI), as well as trends of the number of events and precipitation amounts belonging to 12 different daily intensity categories. For an easier understanding of geographical patterns, we set up a gridded data set in terms of anomalies, with a spatial resolution of 0.1°. All the statistics were analysed for trend over the entire period spanned by the data and on subperiods of variable length. On regional average, we found a weak decrease in TP (about 1%/decade with respect to the 1971–2000 mean) over the entire studied period (1922–2009), which was statistically significant only in spring. Gridded data show that the decrease is related to a reduction in the number of WD in the eastern part of the study area, and a decrement in PI in the western part, with orography playing a clear role in this differentiation. On a daily scale, trends of the strongest events present scarce spatial coherence and are only locally significant, however the results are highly dependent on the period analysed. Comparisons with previous low-resolution studies on the same area underline the importance of a high-resolution data set in characterizing spatial variability of climatic trends in precipitation. Copyright © 2011 Royal Meteorological Society

KEY WORDS daily precipitation; Alps; homogenization; precipitation intensity

Received 3 September 2010; Revised 15 March 2011; Accepted 16 April 2011

1. Introduction

Precipitation is one of the most challenging variables in climate sciences; it involves many different spatial scales and disciplines, from cloud microphysics to synoptic meteorology, and it has a crucial influence on the biosphere and human activities. Understanding the characteristics of its variability, both in short and long timescales, is becoming a priority for researchers, especially in the context of an unprecedented global climate change.

The Alps have been defined as the 'water tower' of Europe (EEA, 2009); the flow of many important rivers (Danube, Rhine, Rhone, Po and so on) depends largely on precipitation amounts in the Alpine chain. So it is fundamental to have detailed information about changes in the water cycle in the Alps, where the temperature has risen at a roughly double rate with respect to the global average over the last century (Böhm *et al*., 2001; Brunetti *et al*., 2006a; Auer *et al*., 2007; Brunetti *et al*., 2009).

Studies on the greater Alpine region (GAR: 4–19 °E, 43–49 °N) highlighted differences in precipitation trends in different zones of the Alps, particularly in areas divided by the ridge of the main chain (Brunetti *et al*., 2006a, 2009). Whereas stations located north of the ridge present some increase in total precipitation (TP) (especially in winter and spring), decreases prevail in the south.

Few studies have tried to analyse precipitation in Alpine areas with a high spatial resolution; for example, Schmidli and Frei (2005) for Switzerland or Ciccarelli *et al*. (2008) for northwestern Italy. However, detailed and reliable information about climatic trends in the eastern part of the Alpine chain is not available in the literature.

Low-resolution analysis revealed no significant trends for TP in the northeasternmost area of Italy during the last century (Brunetti *et al*., 2001a, 2004, 2006b), but a significant decline in the number of wet days (WD) was found (Brunetti *et al*., 2001a, 2004). More interesting conclusions were drawn for daily data, with a highly significant increase in very intense precipitation, both for the number of events and their contribution to total amounts (Brunetti *et al*., 2001a, 2004). This is a common result for many areas of the world, like South America (Haylock *et al*., 2006), conterminous United States (Groisman *et al*., 2004; Higgins *et al*., 2007) and Europe as a whole (Klein-Tank and Können, 2003); furthermore, it is an expected consequence of global warming (IPCC, 2007). However, the spatial coherence of these increases is generally low, suggesting that a

* Correspondence to: M. Brunetti, ISAC-CNR, via Gobetti 101, I-40129 Bologna, Italy. E-mail: m.brunetti@isac.cnr.it

higher resolution is needed to assess completely the behaviour of heavy rainfall. Besides spatial variability, the trends also strictly depend on the period studied and the season.

High-resolution studies in Europe draw a very heterogeneous picture regarding the trends of events above the 90th percentile of the daily precipitation distribution. A general decrease was found in the northeastern Iberian Peninsula for the period 1955–2006 (Lopez-Moreno *et al*., 2010), whereas in Switzerland, during the 20th century, there was a clear tendency towards a diffuse increase in autumn and winter (Schmidli and Frei, 2005). In Italy, in the southern region of Calabria, intense events suffered a marked reduction on a yearly scale over the period 1923–2006 (Brunetti *et al*., 2011), but from 1951 to 2004 in the northern part of the Apennines the decrease was limited to winter and spring and there was an increase in summer (Pavan *et al*., 2008). This kind of analysis over long periods (starting before 1950) is actually quite rare in the literature, as it is generally hampered by the poor availability of long daily series (Alexander *et al*., 2006).

Daily precipitation data in Italy are abundant, especially since the end of World War I, when a national Hydrographic Office was set up. Moreover, part of this data has been already digitized. Since the beginning of the 2000s, managing competences over the data have been regionalized, and the Hydrographic Office has been closed, so the availability of digitized data is now highly dependent on regional politics and resources; the meteorological services of the two main provinces in our study area have digitized and archived a total of 255 series for precipitation. Some national network of weather stations is still present in Italy (e.g. the air force network, the electrical board network, etc.), but its spatial density and temporal coverage are substantially reduced.

In spite of good data availability, only a small fraction of the Italian records has undergone detailed homogeneity control procedures; the lack of such procedures can alter or even hide real climatic trends (Alexandersson, 1986; Peterson *et al*., 1998; Aguilar *et al*., 2003).

The purpose of this paper is to partially fill the lack of high-resolution data for the eastern Alps, by presenting a homogenized, high-resolution data set of daily precipitation for the central-eastern part of the Italian Alps. First, we describe the homogenization procedure and the gap-filling technique adopted, then trends of TP, WD, average intensity (PI) and 12 different intensity categories are analysed. Ten categories are defined by thresholds based on deciles, and applied both to the number of events falling into each category (NPC1,. . ., NPC10) and the total quantity of precipitation associated to those events (PC1,. . ., PC10). For instance, NPC1 is the number of events below the 10th percentile, NPC2 is the number of events between the 10th and 20th percentiles, and NPC10 is the number of events above the 90th percentile. We defined two more categories to represent intense events, NPC95 and NPC99 (with respective PC95 and PC99), which summarize the events above the 95th and the 99th percentile.

2. Study area

The study area comprises the administrative region of Trentino – Alto Adige/Südtirol and surrounding zones (provinces of Vicenza and Belluno towards the east, provinces of Brescia, Sondrio and the easternmost part of the Grisons canton in Switzerland towards the west), making a total of almost 20 000 km^2 (i.e. about 10% of the total area of the Alpine chain). This region is located in a transition zone between the climate of the Southern Alps (more influenced by the Mediterranean Sea) and that of the Northern Alps (more continental-like with influences from the Atlantic Ocean), where the Alpine chain reaches its largest meridional width (Brunetti *et al*., 2006a). A large valley (the Adige valley), hosting the most populated cities (Trento and Bolzano/Bozen), lies in the middle of the region with a nearly north–south orientation, whereas the main mountains ranges are located towards the western and eastern borders. The complexity of the topography, with elevations varying between about 50 and 3900 m, allows the coexistence of many different microclimates; in the space of only 100 km both very wet (more than 1500 mm/year) and very dry (less than 500 mm/year) climates are present (Figure 1), making this one of the most heterogeneous areas in Europe with regard to precipitation. Furthermore, the interannual variability of precipitation amounts in the same region has been recognized as the highest on a continental scale, particularly in winter (Bartolini *et al*., 2009). For these and other reasons our study area is considered to be one of the most interesting in the GAR also for regional climate projections (Smiatek *et al*., 2009).

We could indeed distinguish between two main climatic zones: one in the south, corresponding roughly to the province of Trento (also known as Trentino), and one in the north, comprising the province of Bolzano/Bozen (also known as South Tyrol). This distinction was made statistically, through an EOF analysis; more specifically, the mean yearly cycles of monthly precipitation over the period 1971–2000 were calculated for each series, then we rotated their first two EOFs (representing 96% of the total variance) using the VARIMAX criteria, which gives more spatially homogeneous EOF patterns (and hence more clearly distinct climatic zones) by maximizing the variance of the loadings (for a complete review on the use of EOF in atmospheric sciences refer Hannachi *et al*., 2007). By using mean yearly cycles, our distinction is based only on the climatology of the stations and not on the spatial coherence of the precipitation anomalies. The mean yearly cycles of the two climatic zones are shown in Figure 1. Both zones have a winter minimum, but the southerly zone has two maxima in spring and autumn, whereas the northerly zone has a single maximum in summer. These behaviours are typical, respectively, of the southern and northern slopes of the Alps (Brunetti *et al*., 2006a).

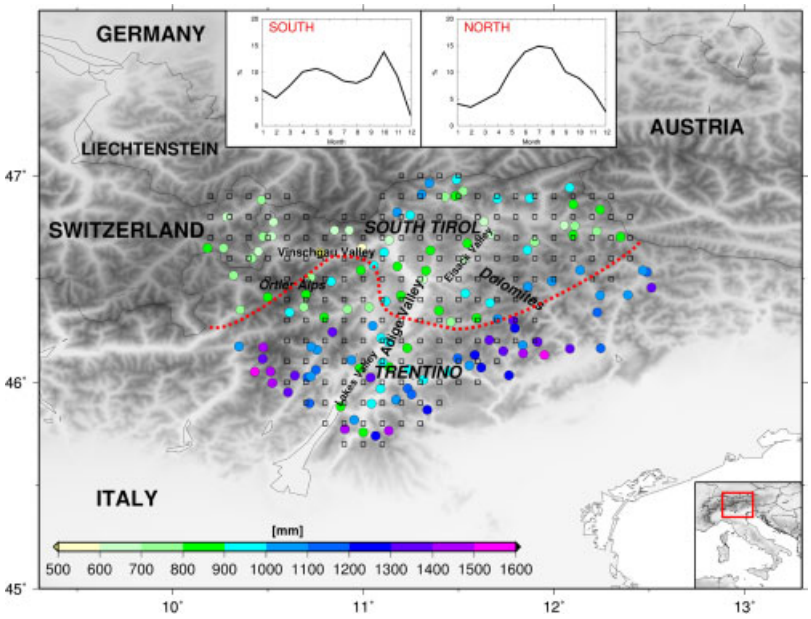

Figure 1. Map of stations used for the analysis (127 stations); colours represent annual mean precipitation over the 1971–2000 reference period, empty squares indicate grid points. Red-dashed line separates the two main climatic zones, for which mean annual cycles over the reference period are plotted (ratios of average monthly precipitation with the average yearly total, in percent). This figure is available in colour online at wileyonlinelibrary.com/journal/joc

3. Data

The data used in this study come from many different sources, but most of the stations were managed by the former Italian Hydrographic Office until the end of the 1990s, when its duties were gradually transferred to regional administrations. Hydrographic Offices of the Autonomous Provinces of Trento and Bolzano/Bozen were the main sources. Data series from stations in the Provinces of Brescia, Sondrio, Vicenza and Belluno come mainly from the Italian electrical board, whereas Swiss series came from MeteoSwiss. Other minor sources were the Environmental Prevention and Protection Agency of the Veneto Region, the former Central Office of Agronomical Ecology (UCEA, now CRA-CMA) and the Italian Air Force.

The data set covers the period 1920–2009 with daily resolution; however, only data since 1922 were analysed as stations with 1920–1921 data are not spatially well distributed.

3.1. Preliminary selection and quality check

The initial number of raw data series of daily precipitation available for the study area was about 300; this was lowered to 200 by excluding series with <20 years of data or characterized by severe quality problems (excessive erroneous outliers or too many and too big inhomogeneities), and by merging the data of stations located very close to each other. Only series with more than 35 years of data and <25% of missing data in the reference period 1971–2000 were used for the analysis (127 series); remaining stations were still useful as references for homogeneity testing and for the reconstruction of missing data.

The average length of the series used for the analysis is 67 years, with 26 series spanning the entire 1922–2009 period. More than half of the stations are located above 1000 m altitude, but only five of them are above 2000 m, the highest one being that of Careser's artificial lake at 2600 m in the Ortler Alps (starting in 1930, one of the highest stations in Europe with at least 80 years of daily data).

Before the homogenization procedure we checked the data for outliers on a daily scale, through comparisons with neighbouring stations, and deleting evident erroneous values or correcting them if possible (such as errors in decimal point positioning).

3.2. Homogenization

As well as for any other meteorological measure, physical signals in raw precipitation data series are often hidden behind non-climatic noise caused mainly by station relocation and changes in instruments, in the environment around the station or in the observing conventions. Daily precipitation series can present inhomogeneities not only in total rain amounts, but also the number of WD. In particular, in this data set in the early years, rainy episodes of several days indicated as a single day event (cumulative data), were relatively common, thus leading to an underestimation of WD and an overestimation of intense events, and therefore introducing significant artificial long-term trends. Inhomogeneities in WD depend also on the threshold used to define them; an excessively low threshold can accentuate the effect of the substitution of a rain gauge, especially when a more sensitive one is installed. For this reason we discarded the events below 1 mm and considered them as non-rainy days.

We checked monthly amounts of TP and WD separately, by means of a multiple application of the Craddock test (Craddock, 1979), which is based on the hypothesis of the constancy of precipitation (or WD) ratios between couples of series. The homogenization approach used in this study was the same as that discussed in Brunetti *et al.* (2006b), but adapted to daily resolution. Each series was tested against the series of the 10 nearest stations, making breaks recognizable without assuming *a priori* homogeneous reference series. Because of the presence of many high-altitude stations in the data set, seasonal-dependent breaks are very common since winter precipitation usually falls as snow; to detect these breaks more easily we applied the homogeneity test by excluding data of the April to September or October to March semester for testing winter or summer, respectively.

Monthly correcting factors were estimated using the neighbouring most correlated series that were homogeneous for a sufficiently long subperiod centred on the break year. The factors related to a certain reference series were calculated by comparing ratios with the inhomogeneous series in a reference subperiod (typically the most recent one without inhomogeneities) and in the subperiod to be corrected. To reduce noise, we used at least three series (when possible) and performed a trigonometric smoothing of the correcting factors. However, when a clear yearly cycle was not evident in the adjustments, we estimated a single factor valid for all months, calculated as the weighted average of the monthly values, where the weights were the ratios between monthly mean precipitation and total annual precipitation. The final correcting factors were the average of single factors relative to each reference series. Daily adjustments were then calculated by fitting a trigonometric function to monthly factors, resulting in 366 daily correcting factors.

Series with inhomogeneities in the number of WDs were not completely discarded, but data in the problematic subperiods were eliminated; typically this consisted of removing the first part of the series, where WDs were underestimated because of the presence of cumulative data. However, in a couple of cases, with particularly favourable conditions, we opted for breaking the series into two homogeneous series.

Only one fifth of the total 200 series were homogeneous, both regarding precipitation amounts and number of WDs. For the others, we recognized and corrected 350 breaks in precipitation amounts (2.8 breaks per homogenized series, equivalent to an average homogeneous period of 33 years between two consecutive breaks) and removed 103 subperiods of data because of inhomogeneities in WDs. Figure 2 shows the distribution in time of the breaks (bar columns); in spite of the lack of detailed metadata, we are able to relate some maxima of the breaks frequency to known historical events. In particular, a large peak is present in 1940, when Italy entered the World War II, and a smaller one in 2000, year of the dismissal of the national Hydrographic Office. The origin of the highest peak (at the end of the 1960s) remains unknown to us.

Figure 2 shows also the time-series of the mean correction for the dataset used for the analysis, i.e. the average of the ratio between the final and the original version of the 127 series, for the yearly data and for winter. Homogenization introduced a weak decreasing trend on the whole period, which becomes relatively strong when looking only at the last 30–50 years, particularly in the cold part of the year: we identified a systematic underestimation of winter and, to a lesser extent, of spring and autumn precipitation (which corresponds to positive corrections) before around 1988. This signal comes mainly from stations located at high elevations, as indicated by the dashed line, which represents the average correction in winter for the stations above 1000 m. We found a possible explanation in a step-like reduction of the fraction of snow in TP, which occurred in the central Italian Alps at the end of the 1980s (Bocchiola and Diolaiuti, 2010), as the measure of snowfall is often affected by relevant underestimation that can reach 80% during strong wind conditions (Goodison *et al.*, 1998), whereas for liquid precipitation wind-induced underestimations hardly ever exceed 20% (Nespor and Sevruk, 1999; Yang *et al.*, 1999). In fact, rain gauges used in Italy are not wind-shielded and therefore are very prone to this problem, especially at high altitudes where snowstorms are more frequent. In other words, by using also low-elevation series as references for high-elevation series, we might have unconsciously corrected (partially) a kind of inhomogeneity that does not depend on changes in the measurement conditions and that in principle is not characterized by sudden breaks. The correction of wind-induced errors goes beyond the scope of this work, but an evaluation of its possible impact on the trends will be given in the Analysis section. By the way, the reduction in snowfall cannot be blamed as the sole cause of the decreasing trend introduced by the homogenization procedure: for instance, a systematic underestimation of about 2%, independent from altitude, was present even in summer between the 1960s and the 1970s (but not in the 1980s).

3.3. Gap-filling procedure

Missing data is an almost unavoidable characteristic of long meteorological series; furthermore we introduced new gaps by deleting periods with a non-homogeneous number of WDs and erroneous outliers. We decided to fill days only when they were part of a partially incomplete month or when they were in the 1971–2000 reference period. The first correction avoids the loss of many valid daily data for which monthly statistics could not be calculated otherwise, the latter provides a common complete period for all series as reference for anomalies and therefore enables a complete gridded data set to be constructed, based on the anomalies method (Mitchell and Jones, 2005), which minimizes the fraction of reconstructed data in trend analysis (see next paragraph).

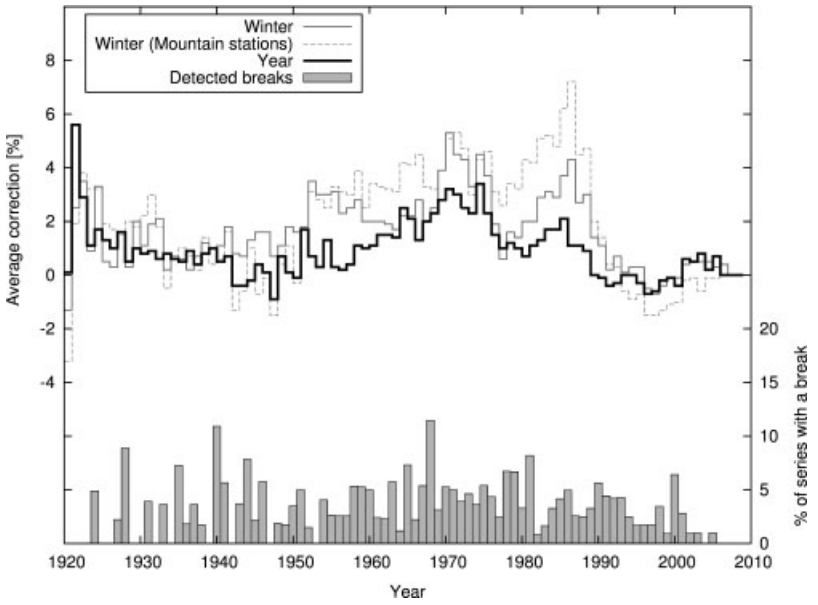

Figure 2. Temporal evolution, on yearly scale and for winter, of the average of the corrections applied through the homogenization procedure to the 127 series used for the analysis; a curve representing mountain stations (above 1000 m) is also plotted for winter. Vertical bars indicate the number of breaks detected in each year (as the percentage relative to the number of available series in that year).

The reconstruction was made by adopting the technique described in Simolo *et al*. (2010), based on a two-step algorithm that avoids the overestimation of WDs and the underestimation of intense events, two common drawbacks of reconstruction methods for daily precipitation. This technique aims to preserve the statistical properties of the series, fitting data with a Gamma distribution, a widely used guess in modelling daily precipitation (Bradley *et al*., 1987; Groisman *et al*., 1999; Jones *et al*., 2004). In the first step rainfall occurrence in the target series is estimated in terms of probabilities, using a weighted average of synchronous values from a cluster of reference series. The weighting factors are functions of relative distance, altitude and angular distribution of the reference stations with respect to the target one. Actual precipitation events are selected using a time-dependent threshold, which discards those low-probability values that most likely correspond to dry events, thereby markedly reducing the error due to false alarms. In the second step, the rainfall amount of previously wet-classified days is reconstructed by a multivariate fit with ordinary least squares, and the generated values are subsequently rescaled to recover the daily probability distribution of the original series; this final operation obviates the systematic underestimation of intense events induced by multi-linear regression (refer Simolo *et al*., 2010 for more details).

The fraction of reconstructed data in the analysed data set of 127 stations is very small (about 2.5%), as can be seen in Figure 3, which describes the temporal evolution of available data.

3.4. Gridding

Interpolation of monthly and seasonal anomalies of the different extracted statistics on a regular grid was an obvious choice for this data set, because the series have variable lengths and are broken by large gaps (only the reference period is complete for all 127 stations). A gridded data set allows us to study the geographical distribution of trends over the entire period for which sufficient data are available (1922–2009).

The grid resolution chosen was 0.1°, near the mean interstation distance (about 7 km). The anomalies were calculated as the ratio (the difference for numbers of days) with respect to average values in the reference period. The use of anomalies instead of absolute values was imposed by the high spatial gradients of the latter compared to the larger spatial coherence of the former (Mitchell and Jones, 2005).

To calculate values for each grid point the stations located at a maximum distance of $2\overline{d}$ were used, where $\overline{d}$ is the mean distance of one grid point from the next one obtained by increasing both longitude and latitude by one grid step. The grid-point series were calculated only if, for every month of every year of the analysed period, at least one station with valid data within $\overline{d}$ or two stations within $2\overline{d}$ were present. This criterion led to the creation of 190 grid points, as represented in Figure 1.

Interpolation was performed by a weighted average with weights given by the product of a radial and an angular weight.

The radial weight of the ith station for the evaluation of the (x,y) grid cell is as follows:

$$w_i^r(x, y) = \exp\left[-\frac{d_i^2(x, y)}{c}\right] \tag{1}$$

with

$$c = \frac{\overline{d}^2}{\ln 2} \tag{2}$$

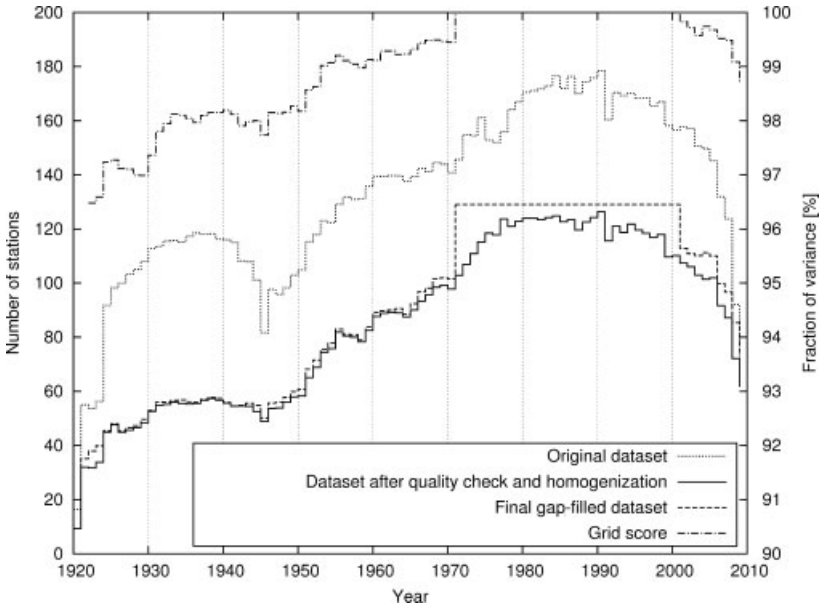

Figure 3. Temporal evolution of data availability.

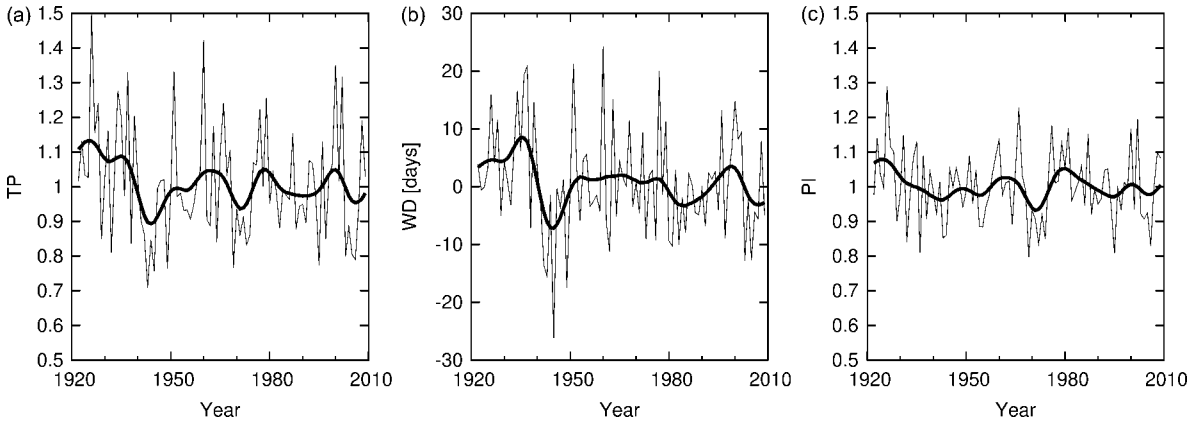

Figure 4. Evolution of regional averages of (a) TP, (b) WD and (c) PI. Thick lines represent the series filtered with a low-pass Gaussian filter (11-year window, 3-year σ). TP and PI are expressed as ratios with respect to the 1971–2000 average, whereas WD are expressed as differences.

where i runs over the stations and $d_i(x, y)$ is the distance between the station i and the point (x,y) for which the local record is being estimated. With this choice of the parameter c, we obtain weights of 0.5 for station distances equal to $\overline{d}$.

The angular weight has the following form:

$$w_i^{\text{ang}}(x, y) = 1 + \frac{\sum_{i=1}^{n} w_i^r(x, y) \cdot [1 - \cos\theta_{(x,y)}(i, l)]}{\sum_{i=1}^{n} w_i^r(x, y)} \tag{3}$$

where $\theta_{(x,y)}(i, l)$ is the angular separation of stations i and l with the vertex of the angle defined at grid point (x,y), and $w_i^r(x, y)$ is the radial weight as defined in Equation (1). The introduction of this angular weight avoids the undesired over-weighting of the areas with the highest station density in the evaluation of the grid cell (Shepard, 1968, 1984; Willmott *et al*., 1985; Efthymiadis *et al*., 2006).

For an estimation of the goodness of grid representation over time, we calculated the 'explained variance' scores, as defined in Efthymiadis *et al*. (2006) for the HISTALP data set. This score is expressed in percent relative to the variance explained by a certain grid point in the reference period (where the score is 100% by definition). For its calculation, values of total seasonal precipitation anomalies for the grid point in the reference period were recomputed using only stations with available data in the target year. In our gridded data set the score never fell below 90% of explained variance, which means that every grid point represents well the precipitation variability over the entire analysed period. Minimum values of the score were always reached before 1950, with the lowest values appearing in spring and summer and near the Italian–Austrian boundary. The evolution of the yearly average score (i.e. the average over the

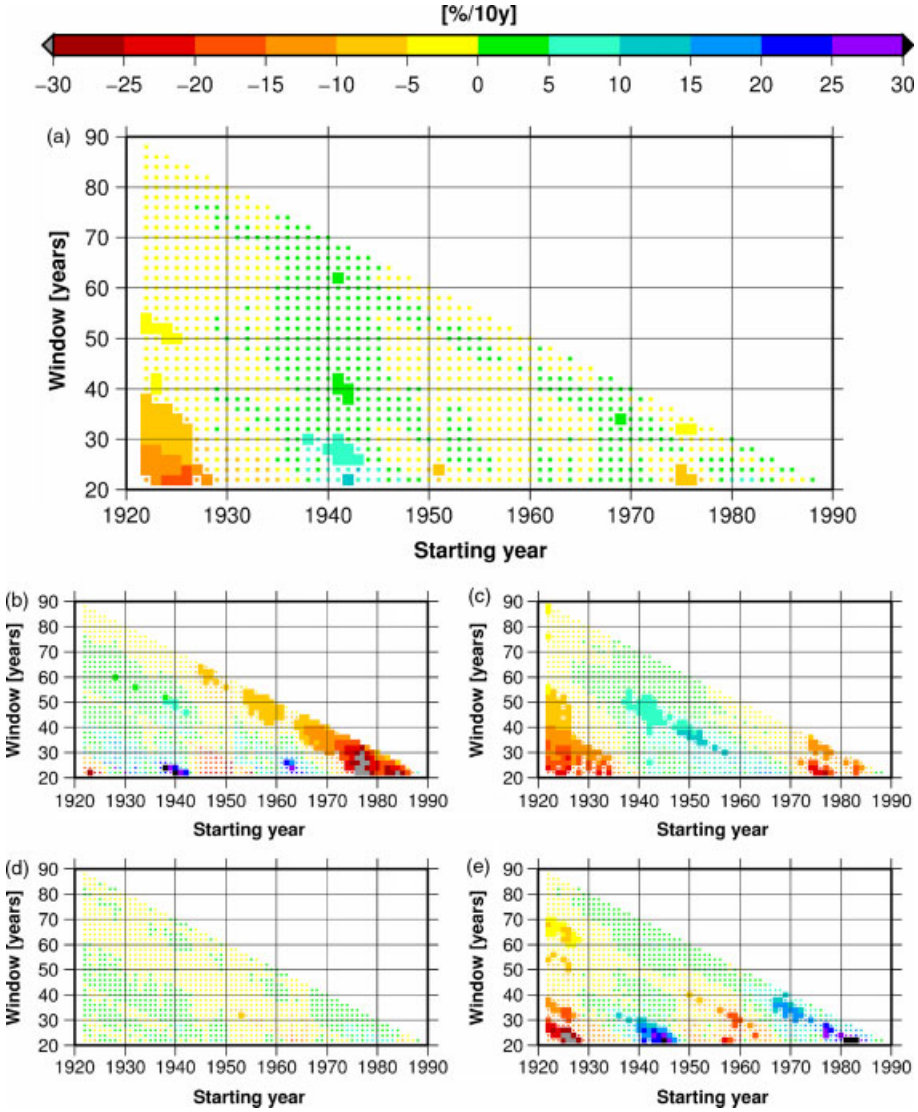

Figure 5. Running-trend analysis for mean regional series of TP: (a) year, (b) winter, (c) spring, (d) summer and (e) autumn. The *y*-axis represents the window width, whereas the *x*-axis represents the first year of the window over which the trend is calculated. Larger squares detect significant trends. This figure is available in colour online at wileyonlinelibrary.com/journal/joc

entire grid) is plotted in Figure 3; qualitatively, it resembles very closely the evolution of the data availability, but a halving of the number of stations from the maximum value yields a reduction of the average score of $<2\%$.

4. Analysis

All statistics were transferred to grid on monthly, seasonal and yearly scales. Here we refer to the meteorological year, which goes from December to November and is subdivided into four seasons: winter (December to February), spring (March to May), summer (June to August) and autumn (September to November). A certain winter or meteorological year is indicated by the calendar year in which it ends.

We analysed linear trends over the entire period as well as over variable temporal windows to capture the whole possible spectrum of significant trends being present in the series. The slopes of the trends were calculated by least square linear fitting, whereas statistical significance was assessed by the Mann-Kendall non-parametric test; the use and computation of this test has been well described by Sneyers (1990). In this study trends were considered significant when the rejection probability of the test's null hypothesis was below 10%.

For the definition of the intensity thresholds we used empirical percentiles, estimated over samples of at least 500 rainy days belonging to the reference period and taken from a window centred in the Julian day for which the threshold was estimated (for each day of the year a different threshold was calculated, the 366 thresholds were then smoothed with a trigonometric function to reproduce a yearly cycle without sudden steps). The thresholds were computed by a linear interpolation of the two values in the sorted data closest to the percentile to be calculated (refer Zhang *et al.*, 2005 for further details). The choice of using empirical percentiles instead

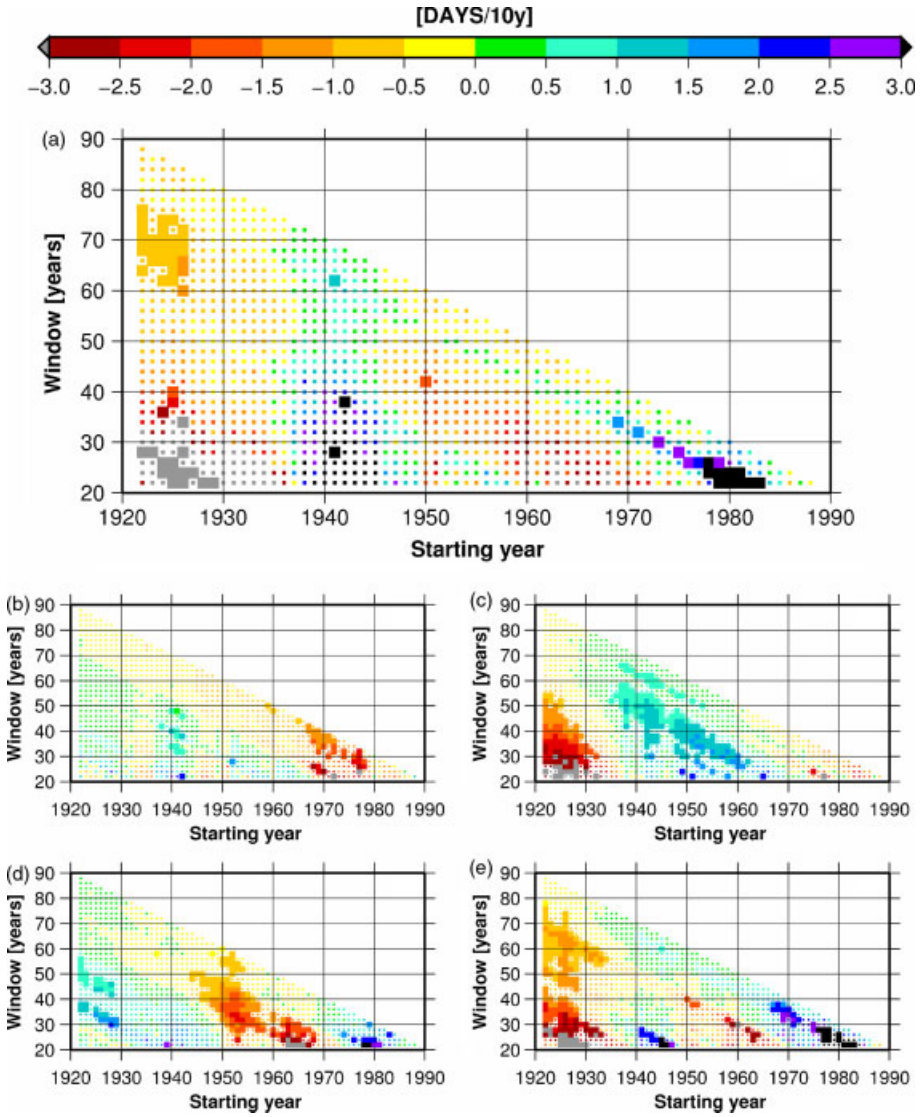

Figure 6. Running-trend analysis for mean regional series of WD: (a) year, (b) winter, (c) spring, (d) summer and (e) autumn. The y-axis represents the window width, whereas the x-axis represents the first year of the window over which the trend is calculated. Larger squares detect significant trends. This figure is available in colour online at wileyonlinelibrary.com/journal/joc

of estimating them from the widely adopted theoretical Gamma distribution (Bradley *et al*., 1987; Groisman *et al*., 1999; Jones *et al*., 2004) is justified by the poor results we obtained for the northwesternmost part of our study area in applying the Lilliefors variant of the Kolmogorov–Smirnov test (Wilks, 1995) for Gamma distribution. The null hypothesis of the test (that the empirical values were extracted from a Gamma distribution) was rejected at the 0.1 significance level in more than 50% of the days of the year for every station of that area in the reference period; in particular, winter daily precipitation did not seem to be adequately represented by a Gamma distribution.

4.1. Regional average

First, we analysed mean climatic trends for the entire study area. The regional average was calculated using gridded values; otherwise sectors with a higher density of stations would have had more influence on the average than sectors with few stations.

Figure 4 shows temporal evolutions of regional yearly TP, WD and PI. A deep minimum is evident in the 1940s, particularly in WD (Figure 4(b)); this is a large-scale feature that can be found in many European historical series (Brunetti *et al*., 2004, 2006a; Pauling *et al*., 2006) and even in hemispherical averages (Bradley *et al*., 1987). Another relatively long dry period is present around 1970, caused by a minimum in PI (Figure 4(c)); this seems to be a more local feature. The wettest period is at the beginning of the series, from the 1920s to 1930s, with the absolute maximum being reached in 1926 both for TP and PI.

Over the full period, the only significant trend detected on a regional scale is a decrease in spring for TP ($-2 \pm 2\%$/decade); this result was not influenced by homogenization. Over shorter periods, significant trends are present for each variable, but still the homogenization

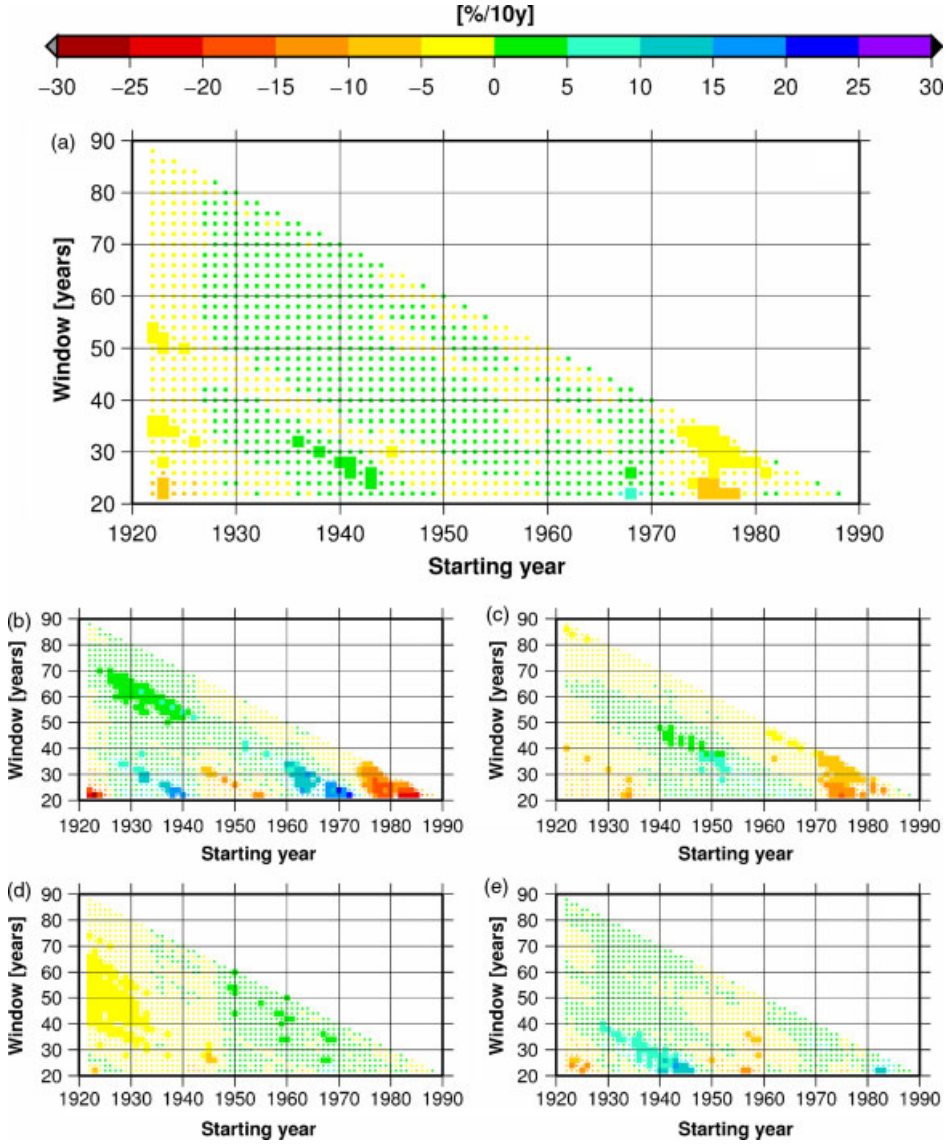

Figure 7. Running-trend analysis for mean regional series of PI: (a) year, (b) winter, (c) spring, (d) summer and (e) autumn. The *y*-axis represents the window width, whereas the *x*-axis represents the first year of the window over which the trend is calculated. Larger squares detect significant trends. This figure is available in colour online at wileyonlinelibrary.com/journal/joc

procedure never played a prominent role for TP on regional scale (although it did on grid-point scale), its contribution to the significant trends being in most cases lower than 10%. As an example, it can be worthy to compare the magnitude of the introduced trend discussed in the Homogenization section with that of the climatic signal found in our analysis: for the last 30–40 years (the most affected period) the former can be estimated as a decrease of about 1%/decade in winter (Figure 2), whereas the latter shows a decrease which lies in the range 5/20%/decade. Conversely, the deletion of data due to inhomogeneities in the number of WD had a strong impact on the regional trends of WD (and therefore also on PI and intensity categories), because the occurrence of cumulative data was much higher in the 1920s and 1930s, thus leading to artificial positive trends in WD and negative trends in PI that were often of the same order (in absolute value) of the actual climatic trends.

The possible influence of the reduction in snowfall at high altitudes is unlikely to have had an important impact on the results. To verify it, we computed two new regional means by averaging the data of the stations located either below or above the 1000 m level; we did not find significant differences in trends between the two subsets.

Figures 5–7 show the results of the running-trend analysis applied to mean regional TP, WD and PI series, respectively, giving evidence of which features are most important in terms of trends at each timescale. A decrease in winter TP is evident over the last 50–60 years, but its contribution to yearly trend is generally negligible (winter being the driest season) and balanced by a growth in autumn. The reduction in spring is highly dependent on the starting year, and is not significant over long periods if the starting year is different from 1922. On the other hand, spring seems to be the season with the highest

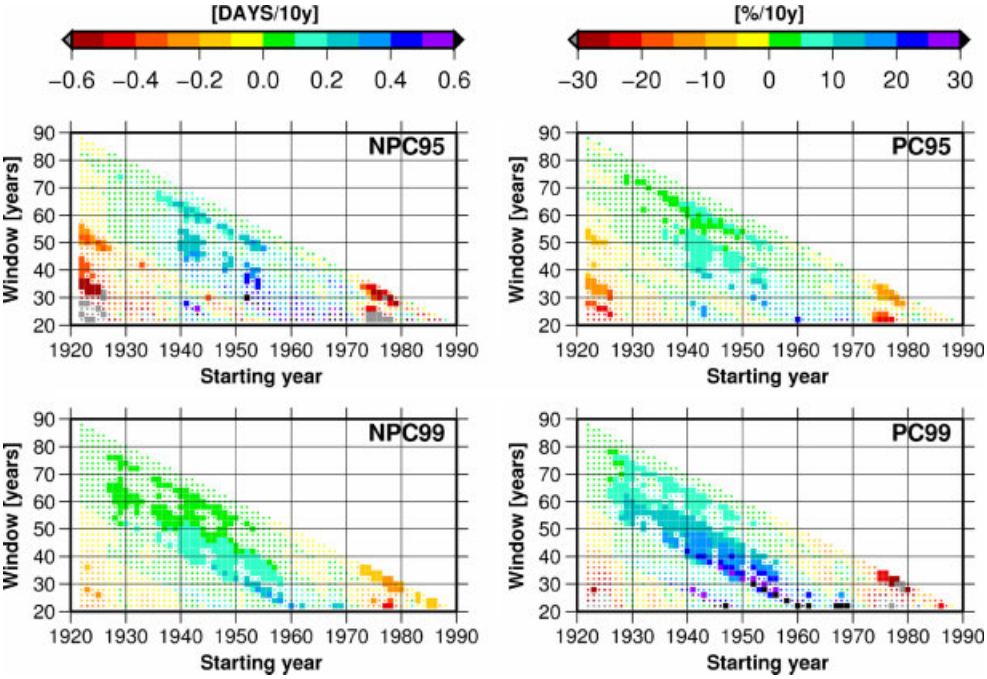

Figure 8. Running-trend analysis for mean regional series of highest intensity categories (yearly values only): (a) winter, (b) spring, (c) summer and (d) autumn. The y-axis represents the window width, whereas the x-axis represents the first year of the window over which the trend is calculated. Larger squares detect significant trends. This figure is available in colour online at wileyonlinelibrary.com/journal/joc

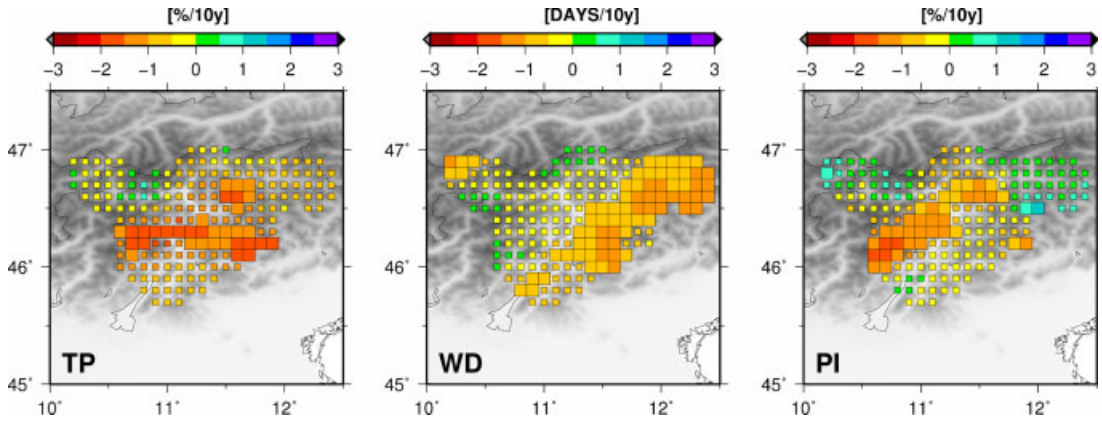

Figure 9. Linear trend maps for yearly TP, WD and PI over the entire period (1922–2009); large squares indicate significant trends. This figure is available in colour online at wileyonlinelibrary.com/journal/joc

impact on yearly trends. For WD, there are significant declines on a yearly scale for subperiods starting in the early 1920s and ending in the 1980s and 1990s (which would not have been detected in the raw data), but not for those ending in the 2000s; this is mainly due to autumn, which presents significant increases in WD starting from around 1970. A similar behaviour is found for PI in winter, where a long-lasting growth is followed by a decrease over the last 35 years, which is present also for the yearly average. In summer significant trends (absent for TP) appear both in WD and PI, counterbalancing each other.

Another example of a trend 'inversion' in the latest decades is given by the highest intensity categories (NPC95, NPC99, PC95 and PC99), shown in Figure 8. The subperiods characterized by the strongest significant increase in intense events are those ending in the 1980s and 1990s. Subperiods ending in the 2000s show trends that are much weaker the more recent the ending year is, consistently with the significant negative trends over the last 30–35 years. In fact, on a regional scale the evolution of intense events is regulated by two short but important periods of maximum frequency (around 1925 and 1980). As for TP, spring is the season that mainly drives the behaviour of yearly totals (not shown).

Results of a previous study that showed a significant increase in the number of events over the 99th percentile in this area (Brunetti *et al.*, 2004) are influenced not only by the ending year of the period it analysed (2002), but also by the starting one, 1921 (not used here), which was the driest year in northern Italy since 1800 (Brunetti *et al.*, 2006a).

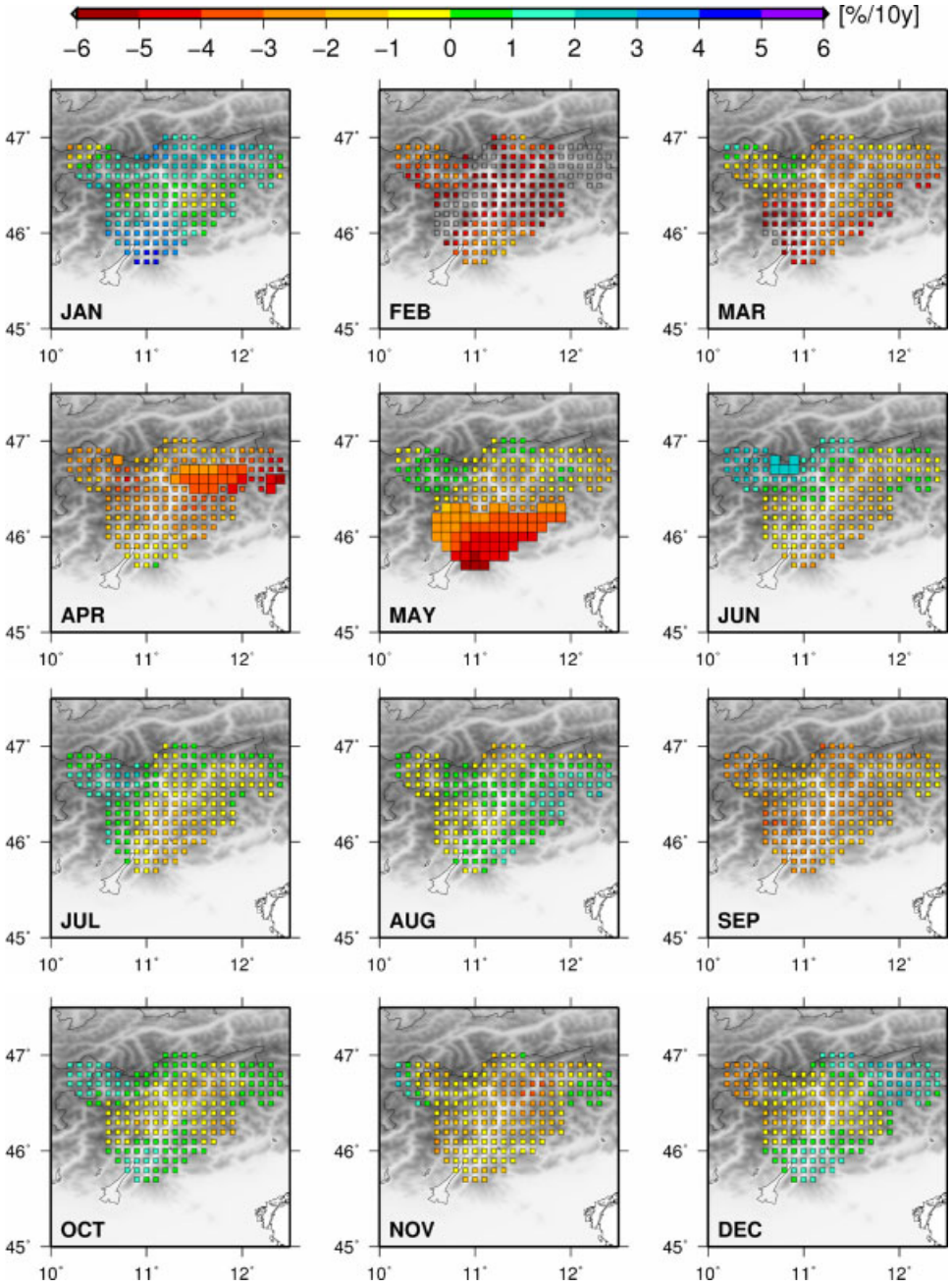

Figure 10. Linear trend maps for monthly TP over the entire period (1922–2009); large squares indicate significant trends. This figure is available in colour online at wileyonlinelibrary.com/journal/joc

4.2. Gridded data

Figure 9 shows the geographical distribution of trend for yearly TP, WD and PI, over the period 1922–2009. Local significant trends are present for each variable, and are dominated by decrements. With the exception of some areas in South Tyrol, the whole region experienced a decline in TP, but only for a few grid points the trends fulfil our requisite for being considered significant. An interesting geographical pattern characterizes WD, suggesting that the Adige valley, along with its physical prolongations (Lakes valley towards southwest and Eisack valley towards northeast), acts as a climatic barrier. To the east of this barrier, WD significantly decrease almost everywhere; to the west, decrements in TP are mainly caused by lowering PI. This characteristic, found thanks to the high resolution of the data set, implies that previous low-resolution studies (Brunetti *et al*., 2001a, 2001b, 2004) slightly overestimated the regional decreasing trend in WD (and consequently underestimated the decreasing trend in PI), because most of the stations used in those analyses are located in the central and eastern parts of the region.

Decreases in TP are concentrated mainly from February to May (Figure 10), whereas some local significant increases took place just north of the Vinschgau valley in June.

The monthly distribution of the declines in WD (Figure 11) is quite similar to that of TP, but with a higher

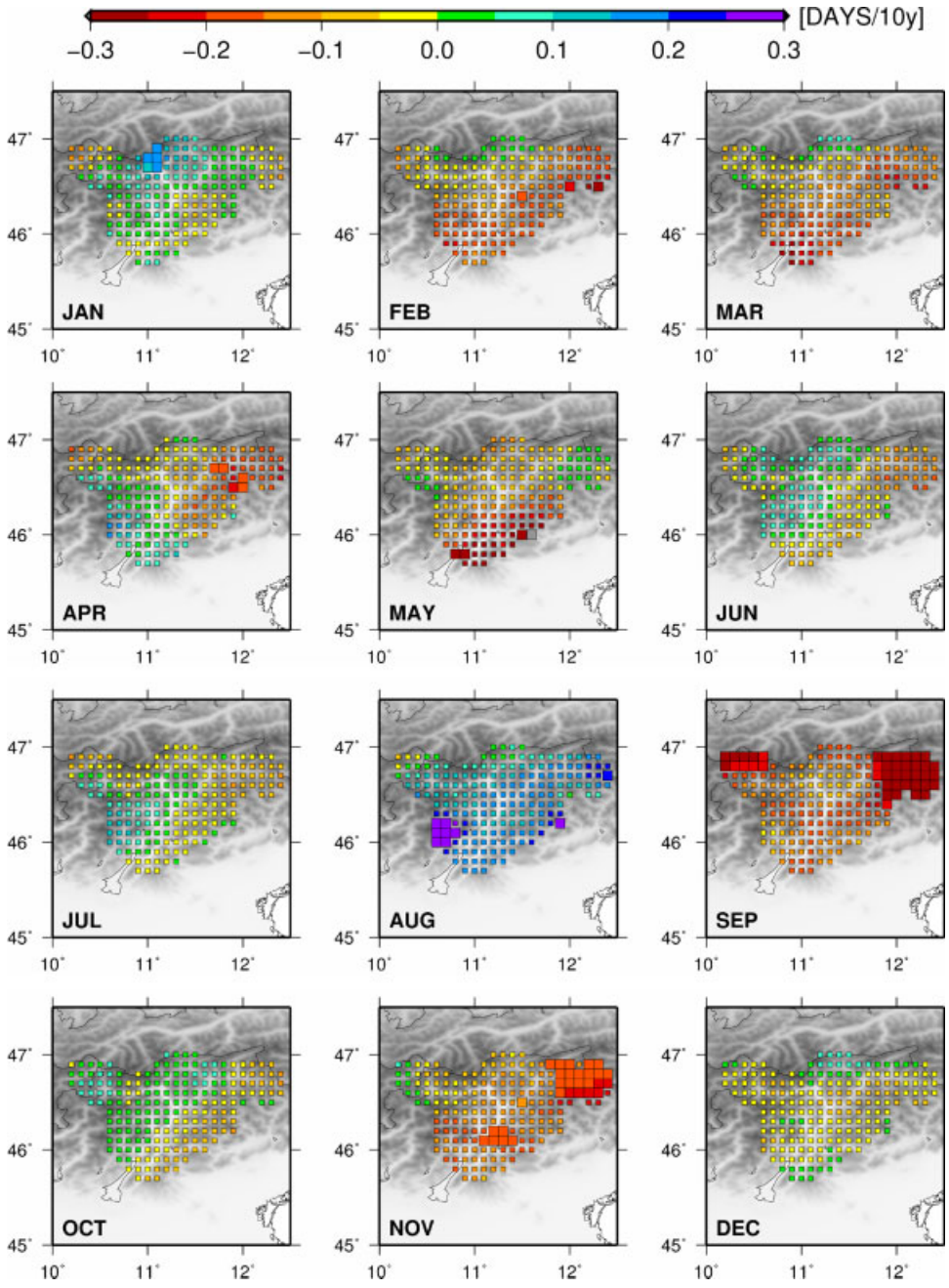

Figure 11. Linear trend maps for monthly WD over the entire period (1922–2009); large squares indicate significant trends. This figure is available in colour online at wileyonlinelibrary.com/journal/joc

contribution by autumn. Locally significant increases are present in August.

For PI (Figure 12), May is again a crucial month in describing negative trends, along with April. On the other hand, in the northwestern part of the region some significant increments appear in June to July, which led to the local growth in TP.

Figures 13 and 14 show trends for intensity categories. The decrease of WD is mainly distributed in the medium-to-high categories (NPC6/NPC9), as well as the decrease in TP (PC6/PC9). Conversely, in the two lowest categories there is a prevalence of increments, both in the number of events (NPC1-NPC2) and their absolute contribution (PC1-PC2), concentrated in the western part of the region. Interestingly, the highest category among the evenly spaced ten, i.e. PC10, is the only one without any grid point with significant trend, although some are present in every season, particularly in summer (decreases in southeastern Trentino and increases in the Vinschgau valley, not shown).

Significant variations in the most intense events (NPC95-99, PC95-99) are limited to few grid points; in particular, in the south of the study area some isolated declines can be seen for NPC95-99, whereas towards the northern boundary some sparse grid points show an increase in PC99. However, as shown in Figure 8, significant trends are present on shorter timescales, but even over temporal windows with significant growth of intense

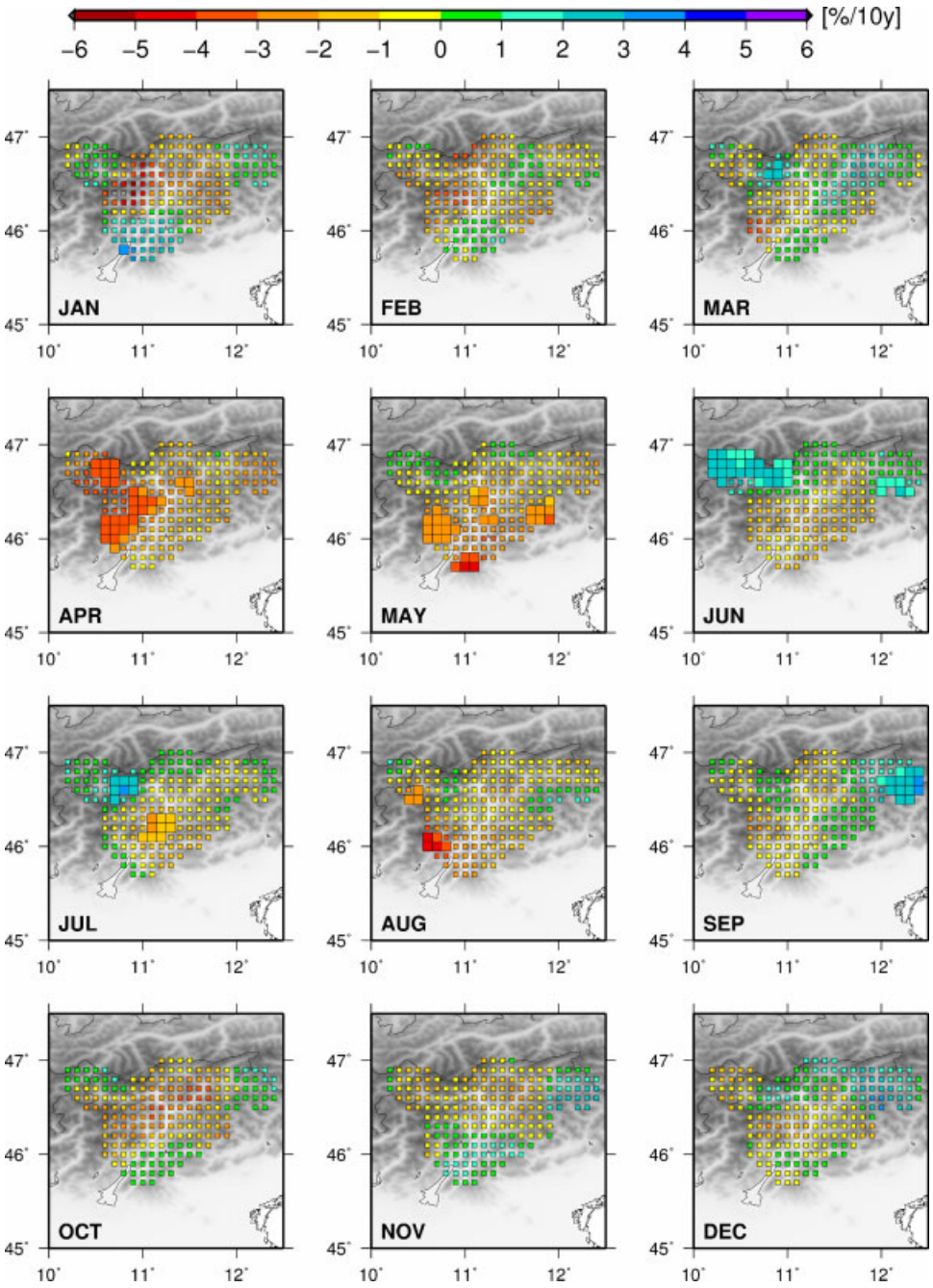

Figure 12. Linear trend maps for monthly PI over the entire period (1922–2009); large squares indicate significant trends. This figure is available in colour online at wileyonlinelibrary.com/journal/joc

events on regional average, there are often some grid points in the south of the region with significant decrements (not shown), underlining the remarkable spatial variability of these statistics; thereafter a high-resolution data set is truly necessary to study them.

5. Conclusions

The collection and homogenization of 200 instrumental series of daily precipitation allowed us to analyse, for the first time, the climatic signals in the eastern part of the Alps with a high spatial resolution, covering the period 1922–2009. Both precipitation amounts and number of WDs were tested for homogeneity on a monthly scale; a total of 350 subperiods were corrected, whereas 103 were discarded because of inhomogeneities in the number of WDs. The homogenization brought noticeable changes in the trends of TP only on a local scale, whereas the deletion of periods characterized by the presence of unmarked cumulative data had a strong impact on the trends of the number of WDs even on the regional scale. Both procedures were fundamental in setting up a reliable high-resolution data set.

Various statistics were extracted from the final subset of 127 homogeneous series, with completed data in a common reference period (1971–2000), and then

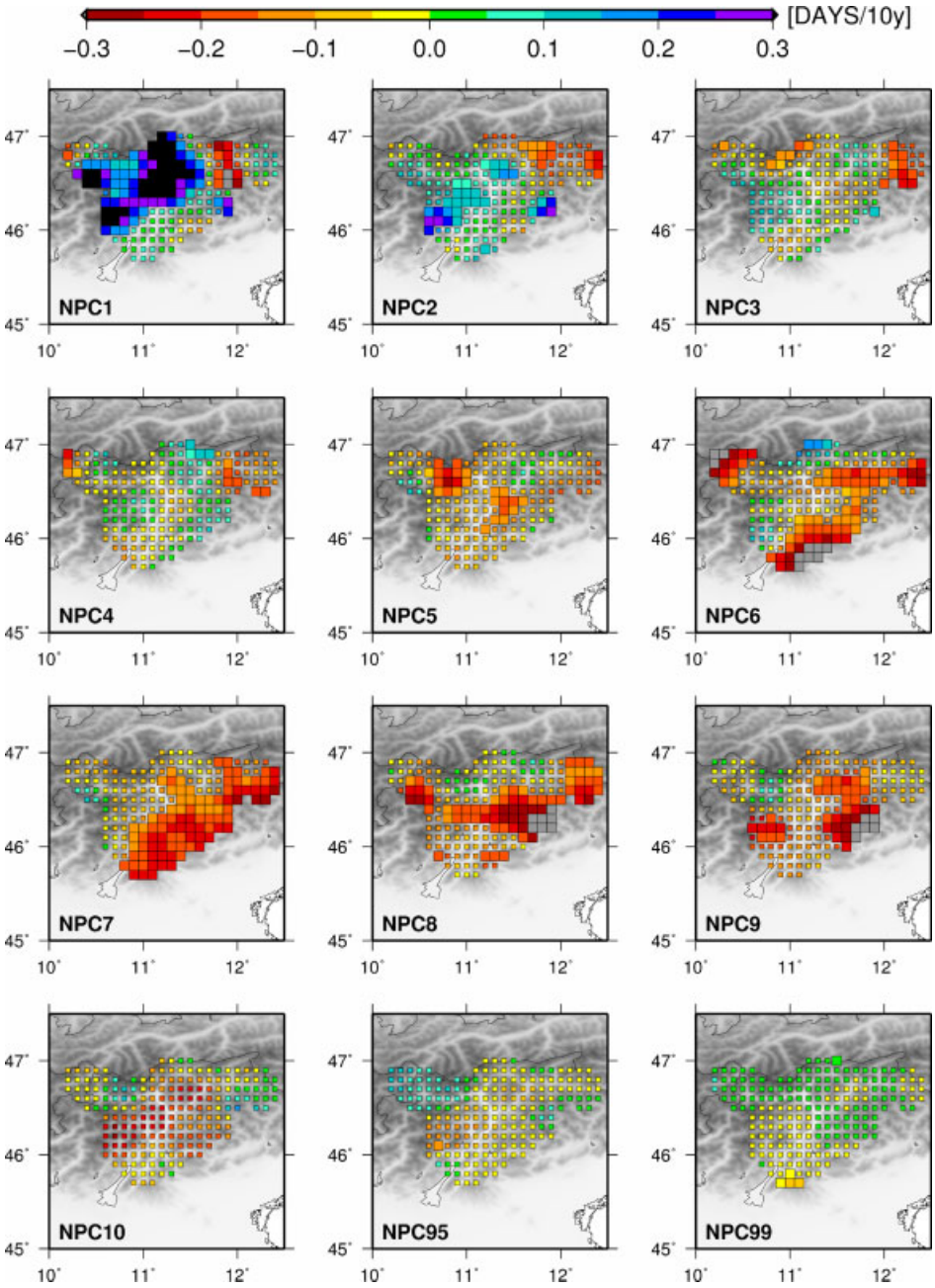

Figure 13. Linear trend maps for the yearly number of events belonging to each intensity category; large squares indicate significant trends. This figure is available in colour online at wileyonlinelibrary.com/journal/joc

interpolated as anomalies over a regular grid with 0.1° resolution. Moreover, a running-trend analysis was performed using regional averages (i.e. the averages of all grid points).

Most of the study area experienced a decrease in yearly TP in the order of 1.0–1.5%/decade, although these trends are only locally significant. The season providing the largest contribution to the decline is spring and, to a lesser extent, winter.

The number of yearly WDs diminished significantly to the east of the Adige valley, whereas significant decrements in the PI occurred mainly to the west.

The decrease in number of WDs is concentrated in the events comprised between the 50th and the 90th percentile of the empirical distribution. Conversely, the lowest categories (below 20th percentile) present diffuse increases in the western part of the region.

The most intense events (over 90, 95 and 99th percentiles) have small trends over the full period analysed, rarely significant even on a local scale. This result might be considered quite surprising, because previous low-resolution studies found very significant growths for the number of events above 99th percentile and for their relative contribution to TP in the northeastern part of Italy over various periods (Brunetti *et al*., 2001a, 2001b, 2004). The running-trend analysis revealed that the last decade was decisive, along with a different choice of the starting year, in reducing these trends to non-significant

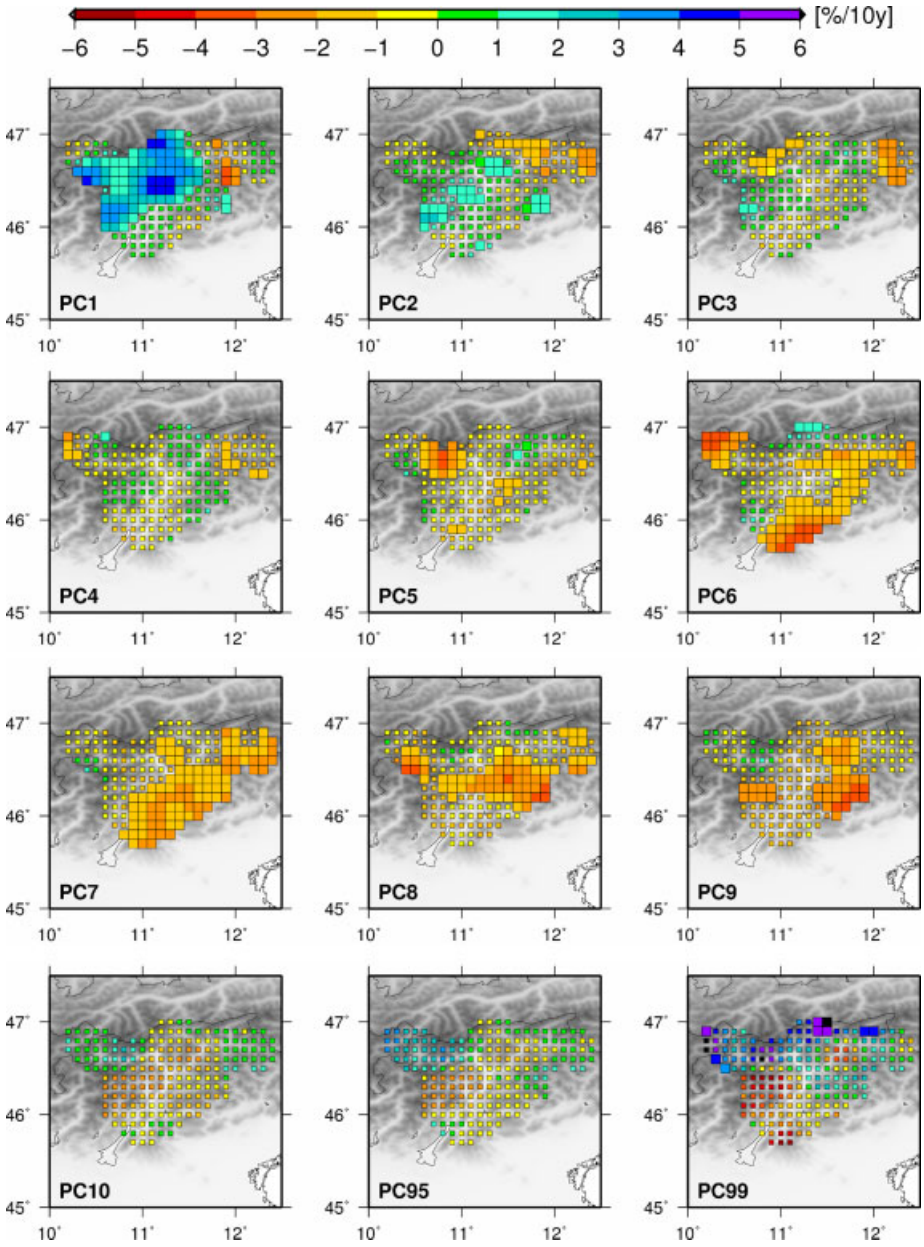

Figure 14. Linear trend maps for the absolute contribution of each category; large squares indicate significant trends. This figure is available in colour online at wileyonlinelibrary.com/journal/joc

values, highlighting the limits in comparing studies based on even slightly different periods and the importance of continuous updates.

Thanks to the high resolution of the data set, we were able to recognize some local topographic influences on the climatic signals, such as the role of main valleys in confining the decrease of WDs, and calculate more precise regional averages with respect to previous low-resolution studies, in which uneven spatial distributions of the stations affected to some extent the results.

Acknowledgements

The research was developed in the framework of the project 'Validazione e downscaling di scenari prodotti con modelli climatici attraverso l'utilizzo di una griglia di variabili meteorologiche ad altissima risoluzione' in the frame of the ISAC-CNR/CMCC agreement. The authors also wish to thank EU-COST-ACTION ES0601 'Advances in homogeneization methods of climate series: an integrated approach (HOME)'. Data were kindly provided by *Meteotrentino* (Ufficio Previsioni e Pianificazione della Provincia Autonoma di Trento) and by the 'Ufficio Idrografico della Provincia Autonoma di Bolzano'.

References

Aguilar E, Auer I, Brunet M, Peterson TC, Wieringa J. 2003. Guidelines on climate metadata and homogenization. WCDMP-No.53.WMO-TD No. 1186. WMO: Geneva.

Alexander LV, Zhang X, Peterson TC, Caesar J, Gleason B, Klein Tank AMG, Haylock M, Collins D, Trewin B, Rahimzadeh F, Tagipour A, Rupa Kumar K, Revadekar J, Griffiths G, Vincent L,

Stephenson DB, Burn J, Aguilar E, Brunet M, Taylor M, New M, Zhai P, Rusticucci M, Vazquez-Aguirre JL. 2006. Global observed changes in daily climate extremes of temperature and precipitation. *Journal of Geophysical Research* **111**: D05109, DOI: 10.1029/2005jd006290.

Alexandersson H. 1986. A homogeneity test applied to precipitation data. *International Journal of Climatology* **6**: 661–675, DOI: 10.1002/joc.3370060607.

Auer I, Böhm R, Jurkovic A, Lipa W, Orlik A, Potzmann R, Schöner W, Ungersböck M, Matulla C, Briffa K, Jones P, Efthymiadis D, Brunetti M, Nanni T, Maugeri M, Mercalli L, Mestre O, Moisselin JM, Begert M, Müller-Westermeier G, Kveton V, Bochnicek O, Stastny P, Lapin M, Szalai S, Szentimrey T, Cegnar T, Dolinar M, Gajic-Capka M, Zaninovic K, Majstorovic Z, Nieplova E. 2007. HISTALP – historical instrumental climatological surface time series of the Greater Alpine Region. *International Journal of Climatology* **27**: 17–46, DOI: 10.1002/joc.1377.

Bartolini E, Claps P, D'Odorico P. 2009. Interannual variability of winter precipitation in the European Alps: relations with the North Atlantic Oscillation. *Hydrology and Earth System Sciences* **13**: 17–25.

Bocchiola D, Diolaiuti G. 2010. Evidence of climate change within the Adamello Glacier of Italy. *Theoretical and Applied Climatology* **100**: 351–369, DOI: 10.1007/s00704-009-0186-x.

Böhm R, Auer I, Brunetti M, Maugeri M, Nanni T, Schöner W. 2001. Regional temperature variability in the European Alps: 1760-1998 from homogenized instrumental time series. *International Journal of Climatology* **21**: 1779–1801, DOI: 10.1002/joc.689.

Bradley RS, Diaz HF, Eischeid JK, Jones PD, Kelly PM, Goodess CM. 1987. Precipitation fluctuations over Northern Hemisphere land areas since the mid-19th century. *Science* **237**: 171–175, DOI: 10.1126/science.237.4811.171.

Brunetti M, Maugeri M, Nanni T. 2001a. Changes in total precipitation, rainy days and extreme events in northeastern Italy. *International Journal of Climatology* **21**: 861–871, DOI: 10.1002/joc.660.

Brunetti M, Colacino M, Maugeri M, Nanni T. 2001b. Trends in the daily intensity of precipitation in Italy from 1951 to 1996. *International Journal of Climatology* **21**: 299–316, DOI: 10.1002/joc.613.

Brunetti M, Maugeri M, Monti F, Nanni T. 2004. Changes in daily precipitation frequency and distribution in Italy over the last 120 years. *Journal of Geophysical Research* **109**: D05102, DOI: 10.1029/2003JD004296.

Brunetti M, Maugeri M, Nanni T, Auer I, Böhm R, Schöner W. 2006a. Precipitation variability and changes in the greater alpine region over the 1800-2003 period. *Journal of Geophysical Research* **111**: D11107, DOI: 10.1029/2005JD006674.

Brunetti M, Maugeri M, Monti F, Nanni T. 2006b. Temperature and precipitation variability in Italy in the last two centuries from homogenised instrumental time series. *International Journal of Climatology* **26**: 345–381, DOI: 10.1002/joc.1251.

Brunetti M, Lentini G, Maugeri M, Nanni T, Auer I, Böhm R, Schöner W. 2009. Climate variability and change in the Greater Alpine Region over the last two centuries based on multi-variable analysis. *International Journal of Climatology* **29**: 2197–2225, DOI: 10.1002/joc.1857.

Brunetti M, Caloiero T, Coscarelli R, Gulla G, Nanni T, Simolo C. 2011. Precipitation variability and change in the Calabria region (Italy) from a high resolution daily data-set. *International Journal of Climatology*, DOI: 10.1002/joc.2233.

Ciccarelli N, von Hardenberg J, Provenzale A, Ronchi C, Vargiu A, Pelosini R. 2008. Climate variability in the north-western Italy during the second half of the 20th century. *Global and Planetary Change* **63**: 185–195, DOI: 10.1016/j.gloplacha.2008.03.006.

Craddock JM. 1979. Methods of comparing annual rainfall records for climatic purposes. *Weather* **34**: 332–346.

EEA. 2009. Regional climate change and adaptation: The Alps facing the challenge of changing water resources. European Environmental Agency (EEA) Report No. 8/2009. DOI: 10.2800/12552.

Efthymiadis D, Jones PD, Briffa KR, Auer I, Böhm R, Schöner W, Frei C, Schmidli J. 2006. Construction of a 10-min gridded precipitation data set for the Greater Alpine Region for 1800-2003. *Journal of Geophysical Research* **111**: D01105, DOI: 10.1029/2005jd006120.

Goodison BE, Louie PYT, Yang D. 1998. WMO Solid precipitation measurement intercomparison, final report. WMO/TD no. 872, WMO. Geneva.

Groisman PY, Karl TR, Easterling DR, Knight RW, Jamason PF, Hennessy KJ, Suppiah R, Page CM, Wibig J, Fortuniak K, Razuvaev VN, Douglas A, Førland E, Zhai PM. 1999. Changes in the probability of heavy precipitation: important indicators of climatic change. *Earth and Environmental Science* **42**: 243–283, DOI: 10.1023/a:1005432803188.

Groisman PY, Knight RW, Karl TR, Easterling DR, Sun B, Lawrimore JH. 2004. Contemporary changes of the hydrological cycle over the contiguous United States: trends derived from in situ observations. *Journal of Hydrometeorology* **5**: 64–85, DOI: 10.1175/1525-7541(2004)005<0064:ccothc>2.0.co;2.

Hannachi A, Joliffe IT, Stephenson DB. 2007. Empirical orthogonal functions and related techniques in atmospheric science: a review. *International Journal of Climatology* **27**: 1119–1152, DOI: 10.1002/joc.1499.

Haylock MR, Peterson C, Alves LM, Ambrizzi T, Anunciação YMT, Baez J, Barros VR, Berlato MA, Bidegain M, Coronel G, Corradi V, Garcia VJ, Grimm AM, Karoly D, Marengo JA, Marino MB, Moncunill DF, Nechet D, Quintana J, Rebello E, Rusticucci M, Santos JL, Trebejo I, Vincent LA. 2006. Trends in total and extreme South American rainfall in 1960-2000 and links with sea surface temperature. *Journal of Climate* **19**: 1490–1512, DOI: 10.1175/jcli3695.1.

Higgins RW, Silva VBS, Shi W, Larson J. 2007. Relationships between climate variability and fluctuations in daily precipitation over the United States. *Journal of Climate* **20**: 3561–3579, DOI: 10.1175/jcli4196.1.

IPCC. 2007. *Climate change 2007: The physical science basis*, Contribution of Working Group I to the Fourth Assessment Report of the Intergovernmental Panel on Climate Change. Cambridge University Press: Cambridge and New York.

Jones C, Waliser DE, Lau KM, Stern W. 2004. Global occurrences of extreme precipitation and the Madden-Julian Oscillation: observations and predictability. *Journal of Climate* **17**: 4575–4589, DOI: 10.1175/3238.1.

Klein Tank AMG, Können GP. 2003. Trendsxs in indices of daily temperature and precipitation extremes in Europe, 1946-99. *Journal of Climate* **16**: 3665–3680, DOI: 10.1175/1520-0442(2003)016<3665:tiiodt>2.0.co;2.

Lopez-Moreno JI, Vicente-Serrano SM, Angulo-Martinez M, Begueria S, Kenawy A. 2010. Trends in daily precipitation on the northeastern Iberian Peninsula, 1955-2006. *International Journal of Climatology* **30**: 1026–1041, DOI: 10.1002/joc.1945.

Mitchell TD, Jones PD. 2005. An improved method of constructing a database of monthly climate observations and associated high-resolution grids. *International Journal of Climatology* **25**: 693–712, DOI: 10.1002/joc.1181.

Nespor V, Sevruk B. 1999. Estimation of wind-induced error of rainfall gauge measurements using a numerical simulation. *Journal of Atmospheric and Oceanic Technology* **16**: 450–464, DOI: 10.1175/1520-0426(1999)016<0450:eowieo>2.0.co;2.

Pauling A, Luterbacher J, Casty C, Wanner H. 2006. Five hundred years of gridded high-resolution precipitation reconstructions over Europe and the connection to large-scale circulation. *Climate Dynamics* **26**: 387–405, DOI: 10.1007/s00382-005-0090-8.

Pavan V, Tomozeiu R, Cacciamani C, Di Lorenzo M. 2008. Daily precipitation observations over Emilia-Romagna: mean values and extremes. *International Journal of Climatology* **28**: 2065–2079, DOI: 10.1002/joc.1694.

Peterson TC, Easterling DR, Karl TR, Groisman P, Nicholls N, Plummer N, Torok S, Auer I, Böhm R, Gullett D, Vincent L, Heino R, Tuomenvirta H, Mestre O, Szentimrey T, Salinger J, Førland EJ, Hanssen-Bauer I, Alexandersson H, Jones P, Parker D. 1998. Homogeneity adjustments of in situ atmospheric climate data: a review. *International Journal of Climatology* **18**: 1493–1517, DOI: 10.1002/(sici)1097-0088(19981115)18 : 13<1493::aid-joc329>3.0.co;2-t.

Schmidli J, Frei C. 2005. Trends of heavy precipitation and wet and dry spells in Switzerland during the 20th century. *International Journal of Climatology* **25**: 753–771, DOI: 10.1002/joc.1179.

Shepard D. 1968. A two-dimensional interpolation function for irregularly-spaced data. In *Proceedings of the 23rd National Conference of the Association for Computing Machinery*. ACM publication P-68, Brandon/System Press Inc: Princeton, New Jersey, 517–524.

Shepard D. 1984. Computer mapping: The SYMAP interpolation algorithm. In *Spatial Statistics and Models*, Gaile GL, Willmott CJ (eds). D. Reidel Publishing Co.: Dordrecht, 133–145.

Simolo C, Brunetti M, Maugeri M, Nanni T. 2010. Improving estimation of missing values in daily precipitation series by a probability density function-preserving approach. *International Journal of Climatology* **30**: 1564–1576, DOI: 10.1002/joc.1992.

Smiatek G, Kunstmann H, Knoche R, Marx A. 2009. Precipitation and temperature statistics in high-resolution models: evaluation for the European Alps. *Journal of Geophysical Research* **114**: D19107, DOI: 10.1029/2008JD011353.

Sneyers R. 1990. On the statistical analysis of series of observation. Technical Note No. 143, WMO: Geneva.

Wilks DS. 1995. *Statistical Methods in the Atmospheric Sciences*. Academic Press: New York.

Willmott CJ, Rowe MC, Philpot WD. 1985. Small-scale climate maps: A sensitivity analysis of some common assumptions associated with grid-point interpolation and contouring. *Cartography and Geographic Information Science* **12**: 5–16, DOI: 10.1559/152304085783914686.

Yang D, Elomaa E, Tuominen A, Aaltonen A, Goodison B, Gunther T, Golubev V, Sevruk B, Madsen H, Milkovic J. 1999. Wind-induced precipitation undercatch of the Hellmann gauges. *Nordic Hydrology* **30**: 57–80, DOI: 10.2166/ nh.1999.004.

Zhang X, Hegerl G, Zwiers FW, Kenyon J. 2005. Avoiding inhomogeneity in percentile-based indices of temperature extremes. *Journal of Climate* **18**: 1641–1651, DOI: 10.1175/jcli3366.1.

